Proceedings of the ASME 2023 International Design Engineering Technical Conferences & Computers and Information in Engineering Conference
IDETC/CIE 2023
August 20-23, 2023 Boston, MA, USA

DETC2023-117126

OPTIMAL SWING ASSISTANCE USING A HIP EXOSKELETON: COMPARING SIMULATIONS WITH HARDWARE IMPLEMENTATION

Salvador Echeveste[1], Ernesto Hernandez Hinojosa[1]

[1] University of Illinois, Chicago

ABSTRACT

Despite tremendous potential, predictive simulations for exoskeleton control tend to overpromise the performance of assistance on walking. The transition from simulation to hardware faces several hurdles such as difficulty representing human-machine interface, an overreliance on intuition, and a lack of exploration in assistive strategies. This work presents a simulation-to-hardware strategy that creates optimized assistance profiles to implement on a hip exoskeleton to assist leg swinging as an intermediary step to improve control strategies for walking. By simplifying the activity we were able to observe a smaller disconnect between simulation and hardware. In addition, the comparison provided insight on the differences between the effectiveness of assistance on frequency of the activity and type of work.

Keywords: rehabilitation robotics, hip exoskeleton, optimization, simulation

1. INTRODUCTION

The use of exoskeletons as assistive devices has become increasingly popular in recent years. In particular, improving how exoskeletons assist people while walking has become a significant area of research. Several different devices have surfaced over the years that provide assistance in a manner that reduces the energy economy [1–3]. However, assistive strategies still cannot fully account for the human-machine interface and in turn, lead to diverging results when carrying over simulation results into hardware [4,5].

Predictive simulations are extremely useful tools in the world of exoskeletons since they allow rapid implementation of control strategies without the need for costly experiments [6,7]. In a digital realm, promising control strategies can be investigated on simpler models by applying them to representations that can mimic the reaction of a user [6, 7]. However, model-based control carried over to hardware often falls short [10]. These models cannot fully capture the complexity of human interfacing with the device and in turn over promise reductions in the energy economy [11]. Therefore, despite a steady increase in the sophistication of simulation technology [8], there is still a gap between digitally optimized results and optimized control implemented in hardware.

There are several reasons why this is a challenging problem to tackle. The objective of representing the physical interactions between a human and an orthotic is difficult to fully grasp in a simulated environment [12,13]. Simulations are meant to simplify the real world to allow an easier exploration of control solutions. Most simulations in the world of robotics that carry over to real-world implementations face a need to be adjusted [14]. One aspect that makes this particularly difficult with orthotics is the human element [12]. Exoskeleton simulations are constantly being improved to better represent their real-world counterpart [15]. Still,

perhaps instead of bringing the simulated world closer to the real world first, it might be necessary to bring the real world closer to the simulated one. Current models might be oversimplified for the task they are trying to mimic, but making the models more complex might compound the difficulty of making a good simulation. Making a simulation more sophisticated requires more computational power or significantly longer simulations. Instead, carrying over to a simpler activity to analyze how current simulated optimized results perform could be beneficial. Stationary leg swinging would allow the activity to come to the model instead of the other way around. The dynamic nature of walking and the need for balance make it complex to represent. Leg swinging utilizes the same hip flexor and extension muscle groups as walking, making it a suitable precursor [16]. A stationary leg swing can also be closely resembled with relatively simple models such as the pendulum model or two antagonistic Hill-type muscle models (Fig. 1); two already common simulation models in the world of assistive robotics. Each muscle model is comprised of a series elastic element (SE), a parallel elastic element (PE), and a contractile element (CE) [17,18].

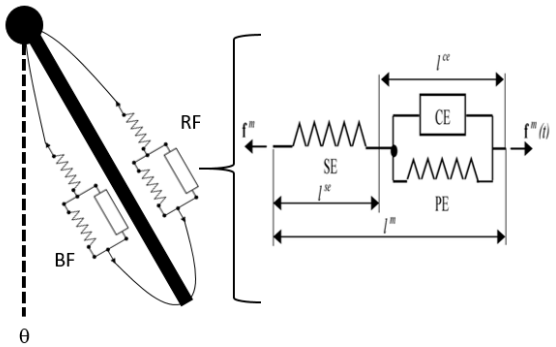

FIGURE 1: PENDULUM SYSTEM WITH ANTAGONISTIC HILL-TYPE MUSCLE MODELS WHERE RECTUS FEMORIS (RF) PRODUCES POSITIVE TORQUE AND BICEP FEMORIS (BF) PRODUCES NEGATIVE TORQUE [19].

Another potential issue causing the gap between simulation and hardware is the heavy reliance on intuition [10]. Despite using the same model, different assumptions will lead to varying results. This can be problematic when carrying over to a physical optimization where the quality of the initial data is critical [20]. Allowing for a simulation to not rely on the manual tuning by the researcher and limiting the number of assumptions could lead to an improved comparison. Implementing a discrete optimization in simulation allows us to do this. A timing based approach has shown the limitation of being prone to discrepancies caused by execution speeds [14]. With discrete optimization of a robust control system, such as a mathematical model relating torque and swing angle, we can allow the simulation to paint a picture for us instead of leading it by the nose [21].

One last potential issue is the lack of exploration within assistive strategies [22]. The design process of exoskeletons often focuses on singular functionality and the development of these devices takes years [10]. This narrows the types of controls that the device can implement and leads to slow progress. This also effectively limits the strength of simulation which is rapid exploration of varying types of control. If the device cannot harvest the strengths of simulation then it limits the potential of finding effective control laws. Therefore, carrying over several types of control laws to explore in hardware would provide an arsenal of assistive strategies to target several types of activities and individuals with varying reactions to assistance.

In order to explore the gap between simulation and hardware this project investigates a side by side comparison of optimized swinging leg torque controllers applied to simulated models and an active hip orthoses. Comparing these two datasets side by side with a simplified activity and a robust simulation could lead to insight on how to improve the simulating process for exoskeletons. In doing so, simulations could provide us a significantly better starting point when we implement and optimize controllers in hardware.

2. METHODS

2.1 Discrete Optimization

In order to avoid relying on intuition about what shape of a discrete torque profile might assist a person best, we turned to simulation to give us an indication of what a promising torque profile shape might be. The ultimate goal of this process was to discover viable torque profiles to pass on to hardware, test them, and conduct a comparison.

The optimization done in simulation allowed for 20 discrete points throughout a forward swing of a pendulum. The pendulum starts at -20° (with respect to the vertical) and swings to 30°, starting and ending with zero velocity. These conditions resemble the desired swing of a leg that will be the center of exoskeleton experiments. In order to observe how different swinging frequencies would affect the torque

profile shape, four different frequencies ranging from 1.32 to 1.97Hz were simulated. These frequencies correspond with observed natural walking frequencies [23].

The process was split into 3 different steps: optimization on a pendulum model to extract the shape of the torque curve, optimization on a muscle model to set the optimal curve parameters, and validation in simulation.

By giving the optimization program the ability to select any torque value within a range discretely ***n*** amount of times throughout the swing, it allows the sequence to draw different pictures according to a desired metric. A similar situation is tested using the more complex model. This model allows us to take a step closer to what we are actually seeking to do: lower the effort of a muscle during a swing. Once shapes are generated by both models they need to be validated against a model that does not have assistance. The reduction in energy or torque is observed and tested for statistical significance. The profiles that perform well at this step advance to hardware.

The torque profiles that come out of simulation are implemented in hardware by coding the mathematical relationship between angles of the swing and torque as they relate to a handful of parameters. Once these are implemented, baseline experiments are conducted to observe if there is a reduction in EMG. Then these are compared to simulated results.

2.2 Simulation

2.2.1 Pendulum Model

Using a pendulum model allows for quicker generation of viable shapes. The pendulum model was represented by the following equations:

$$\dot{x}_1 = x2 \quad (1),$$

$$\dot{x}_2 = -\frac{g}{L}\sin(x1) + \frac{u}{mL^2} \quad (2),$$

where x1 is angle, x2 is angular velocity, g is gravity (9.8m/s/s), L is length of the pendulum (.365m), m is mass of the leg and u is the control or torque applied in Nm. The length and mass chosen were derived from anthropometric data [24].

Several cost functions were explored to produce as many viable torque profiles to carry on to further steps. The investigated cost functions included:

- Root mean squared of torque
- Peak torque
- Energy
- Jerk
- Momentum
- Impulse

The torque profiles produced by this model provided insight into the types of shapes that could do well in a more complex model. Analysis on the torque profiles was conducted to extract the tunable parameters to be optimized on a muscle model.

2.2.2 Hill-type Muscle Model

While the pendulum is very useful for its simplicity, it lacks the concept of using antagonistic energy dependent components. Simulated muscles (Fig. 1) are a better indication of what might be useful to implement on a person because the metrics associated with them are dependent on activation time and the reduction of simulated biological torque. For these sets of simulations there were two different focuses for exploration.

The first involved carrying over the shapes developed with the simpler model through a parametrized version of the relationship between torque and angle. In an attempt to simplify the implementation on hardware, the number of parameters used to represent each profile was kept to a minimum. The number of parameters varied from 3 to 6. Parameters revolved around torque magnitudes and timing with relation to angle.

The second focus allowed for the exploration of a discrete optimization of the HIL Muscle Model using a weighted cost function. Since this type of simulation involved the interaction between two systems, elements from both were represented when seeking an optimal solution (motor torque and biological torque). The cost function therefore allowed for both motor power and biological torque to be optimized with a heavier emphasis on the biological component. This optimization problem is shown in equation 3;

$$\min_{\boldsymbol{\tau_m}} w * \int \tau_b^2 \, dt + (1-w) * \frac{\boldsymbol{\tau_m}^T \boldsymbol{\tau_m}}{\Delta t} \quad (3),$$

where $\boldsymbol{\tau_m}$ is a vector containing the 20 discrete motor torque values and τ_b represents the biological torque given from the muscle model. Varying values of *w* were tested.

The muscle activation was modeled using a PID controller to stimulate two antagonistic muscles. The PID controller produced a stimulation signal by trying to minimize the error between current angle and a desired angle equal to the maximum forward position. Positive torque would be generated by a simulated rectus femoris and negative torque was generated using a simulated bicep femoris. The respective muscle parameters for each were implemented from established HIL muscle models [18].

In order to carry over the simulation profiles into hardware, the successful candidates were fitted to a mathematical relationship corresponding angle input to a torque output. These relationships were meant to be as simple as possible to observe parallels between simulation and hardware easily.

2.2.3 Simulation Validation

Performance of the torque profiles produced by the HIL muscle model were evaluated against a simulation with no assistance (pure simulated biological torque). The root mean squared of the differences between the two simulations was used as this performance.

$$PR = \frac{RMS(\tau_b) - RMS(\tau_{sim})}{RMS(\tau_{sim})} \quad (4)$$

This metric is represented mathematically by equation 4, where τ_{sim} is the biological torque of the non-assisted profile, and τ_b is the biological torque of the assisted profile.

2.2.4 Positive vs General Work

Another concept of interest was comparing positive versus general work. Assistive forces for an exoskeleton are typically associated to be positive work, or that which aligns the torque with the direction of travel. In other words if the person is moving their limb with positive velocity then assistive forces would supply positive torque. However, when there is a limit on the range of motion it might be counterproductive to supply excessive torque if the person is desiring their limb to slow down, indicating a need for negative work. The search for an ideal torque profile is then split in two: optimization that allows for general work, no restrictions on torque values, and optimization that allows for only positive work. Both were explored in simulation and carried over in parameterized versions to hardware. Comparison of the effects were analyzed in simulation and hardware metrics.

2.3 Hardware

2.3.1 Device

The device used to supply the assistance was a hip exoskeleton consisting of a BLDC motor and a series of straps. The control system consisted of a raspberry pi that received angle data from a rotary encoder and supplied a torque command to an AK70-10 T motor. Torque was communicated using CAN bus protocol. Proper safety measures were implemented with an emergency stop and software torque cutoffs. The device is shown in Fig. 2.

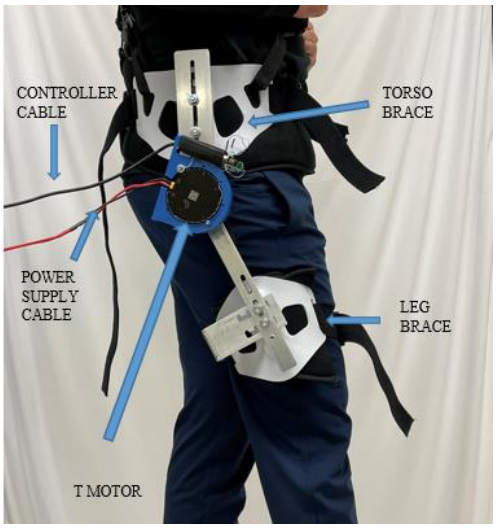

FIGURE 2: MAIN COMPONENTS OF THE HIP EXOSKELETON DEVICE

2.3.2 Controller

The level of assistance was dictated by torque control abiding by the aforementioned mathematical relationship between torque and angle. This relationship simplified the manner of control by creating parameters that focus on 3-6 critical features of the torque profile (torque magnitudes and locations). In order to only apply torque during the forward swing, a finite state machine was implemented. The state machine had two different states representing forward and backward swing. Transitions were triggered with a change in velocity direction derived from the encoder.

2.3.3 Experimental Procedure

In order to measure the effectiveness of each torque profile on hardware, the muscle activity of two muscles was measured. The rectus femoris and the bicep femoris of the swing leg were equipped with Delsys sensors.

Before applying any assistance torque, EMG activity was collected for 3 trials of 2 minutes each.

These initial data collection sessions served as insight into how long a data collection session should last to produce a good comparison metric. Once processed, the data indicated that EMG average stabilizes around 20 seconds of data collection and fatigue sets in around 90 seconds. An ideal capture time of 30 seconds was selected for each condition.

Before swinging with assistance the subject was asked to swing with no exoskeleton on (NE) and with zero assistance (ZA). These would serve as the comparison baseline to measure performance. In addition, the maximum voluntary contraction (MVC) was taken for each muscle to normalize the data.

The swing amplitude was confined to -20 to 30 degrees using physical bumpers on a structure. A metronome was used to promote the subject to swing at the desired frequency. The upper body was confined using a physical structure. The physical structure is represented in Fig. 3.

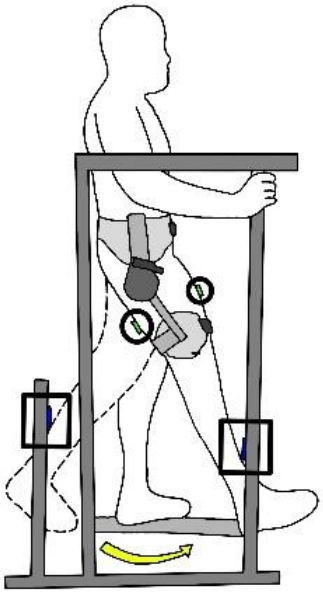

FIGURE 3: ILLUSTRATION OF THE PHYSICAL STRUCTURE AND EXPERIMENTAL SETUP. SHAPES INDICATE KEY FEATURES; SQUARES HIGHLIGHT BUMPER LOCATIONS WHILE CIRCLES SHOW SENSOR PLACEMENT

Each torque profile was applied twice to the subject (male, 80kg) and EMG data was collected. This was done for all 6 torque profiles.

2.3.4 Data Processing

The EMG data collected from both muscles was processed in MATLAB. Each EMG signal was rectified, smoothened, and normalized against the MVC. For each torque profile, the assistance data (AP) was compared to the non-assisted data (NA) by taking the percent difference of a combined representation of muscle activity. The representation averaged out the root mean squared of the rectus femoris and the bicep femoris.

$$\%\, difference = (AP - NA)/NA \qquad (5)$$

3. RESULTS AND DISCUSSION

3.1 Simulation Results

3.1.1 Pendulum Model

Most of the shapes produced by the cost functions implemented in the pendulum model converged to a similar profile. This being the case, one of the metrics selected to advance was the root mean squared of torque. Fig. 4 represents the shape produced by this cost function, referenced in the future as RMS.

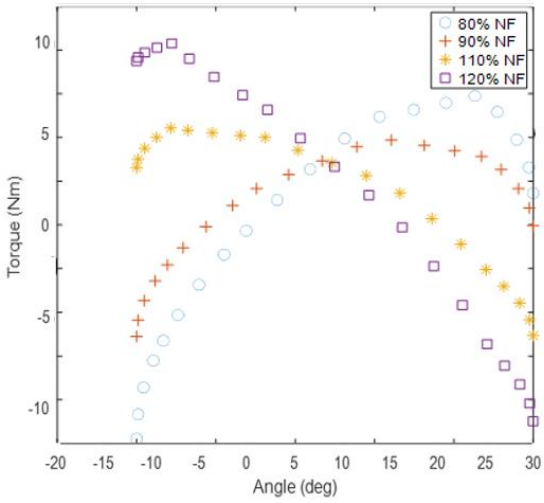

FIGURE 4: TORQUE VS ANGLE RELATIONSHIP OF THE RMS TORQUE PROFILE OF FOUR DIFFERENT SWING FREQUENCIES CALCULATED FROM NATURAL FREQUENCY (NF)

This profile was carried over to be optimized with a muscle model by fitting the relationship between torque and angle with a four parameter relationship. The parameters represent the 3 values of torque and a location. These values include the value found at lowest angle (P1), peak torque value (P2), and torque value found at highest angle (P3) and location of the peak torque (L). The values are then connected with a

linear relationship. The fitting of the torque profile is represented in Fig. 5.

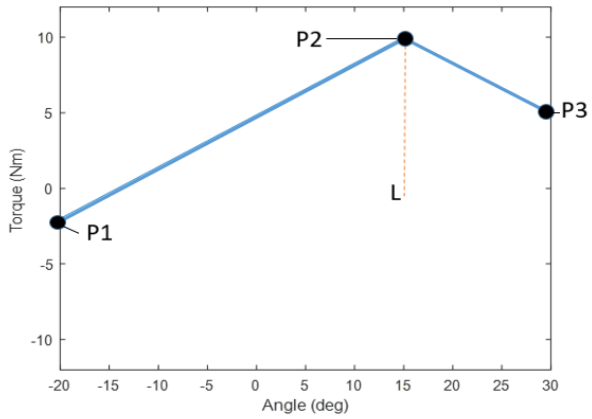

FIGURE 5: PARAMETERIZATION OF THE RMS PROFILE WITH 4 VALUES WHERE P1, P2, AND P3 REPRESENT TORQUE CHECKPOINTS ALONG THE SWING; L REPRESENTS LOCATION OF THE CENTER TORQUE VALUE

The only other metric that did not converge to the RMS equivalent shape was the cost function that minimized peak torque. This produced a flatter association between angle and torque that can be observed in Fig. 6. This profile is dubbed PKK for reference.

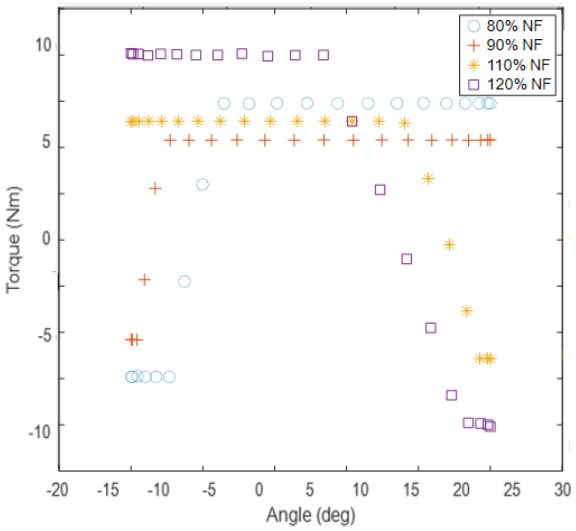

FIGURE 6: TORQUE VS ANGLE RELATIONSHIP OF THE PKK TORQUE PROFILE OF FOUR DIFFERENT SWING FREQUENCIES CALCULATED FROM NATURAL FREQUENCY (NF)

Similar to RMS, this profile was fitted to be optimized with the muscle model. Three parameters were used for this profile. They consisted of initial torque value (V1), later torque value (V2), and the angle at which they switch (S). A visual example of this can be observed in Fig. 7.

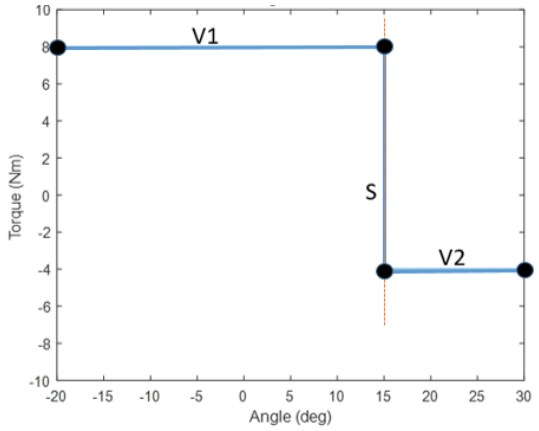

FIGURE 7: PARAMETERIZATION OF THE PKK PROFILE WITH 3 VALUES WHERE V1, AND V2 REPRESENT TORQUE MAGNITUDES AND S REPRESENTS LOCATION OF THE SWITCH

3.1.2 HIL Muscle Model

The discrete optimization of the muscle model using the weighted cost function produced a third type of profile. This torque profile can be observed in Fig. 8 and is dubbed DISMM.

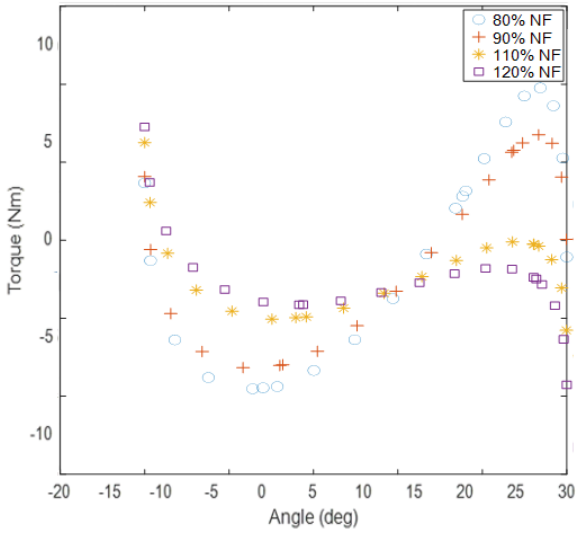

FIGURE 8: TORQUE VS ANGLE RELATIONSHIP OF THE DISMM TORQUE PROFILE OF FOUR DIFFERENT SWING FREQUENCIES CALCULATED FROM NATURAL FREQUENCY (NF)

Fitting this profile was simplified to 6 parameters, four values of torque magnitude (D1, D2, D3, and D4) and 2 locations (C1, and C2). These are visually represented in Fig. 9.

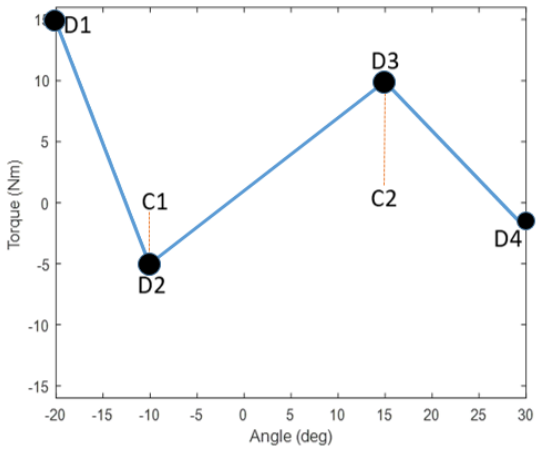

FIGURE 9: PARAMETERIZATION OF THE DISMM PROFILE WITH 6 VALUES WHERE D1-D4 REPRESENT TORQUE MAGNITUDES AND C1-C2 REPRESENT LOCATIONS

Each of these profiles have a positive work only counterpart. To label appropriately, PW is added to each to dictate the distinction. Therefore the 6 profiles that carried over to validation were RMS, PKK, DISMM, RMS-PW, PKK-PW, and DISMM-PW.

3.1.3 Software Validation

Each of the 6 profiles were validated in simulation by comparing the root mean squared of their biological torque component against the root mean squared of the biological torque of a simulation with no assistance. The percent change in the biological torque was then calculated for each profile and used as the metric to compare against.

TABLE 1. PERCENT CHANGE IN BIOLOGICAL TORQUE

	80% NF	90% NF	110% NF	120% NF
RMS	-37.03%	-31.45%	-15.86%	-20.72%
PKK	-28.03%	-20.66%	-4.21%	-9.07%
DISMM	-41.55%	-29.06%	-11.10%	-17.69%
RMS-PW	-37.62%	-27.36%	-15.85%	-20.75%
PKK-PW	-33.31%	-4.00%	-10.41%	-8.91%
DISMM-PW	-33.02%	-22.34%	-7.35%	-15.19%

Table 1 shows the calculated metrics for each profile across all four frequencies. All profiles led to a statistically significant ($p<.05$) reduction in the biological torque of a single swing.

3.2 Hardware Results

3.2.1 No Exoskeleton Metric

After processing all EMG signals, a metric representing the reduction of EMG was calculated for each profile at each swing frequency.

TABLE 2. PERCENT REDUCTION OF NORMALIZED EMG COMPARED AGAINST FREE SWINGING

	80% NF	90% NF	110% NF	120% NF
RMS	-27.87%	8.14%	-17.59%	-33.81%
PKK	-16.38%	-28.69%	-33.35%	-26.49%
DISMM	-22.17%	-23.03%	-31.15%	-35.67%
RMS-PW	-26.34%	14.51%	-28.95%	-33.95%
PKK-PW	-19.14%	-29.00%	-27.44%	-34.93%
DISMM-PW	-22.29%	-3.92%	-33.21%	-35.88%

This metric represented the change in muscle activity between free swinging and swinging with assistance with a normalized representation of both muscles. Table 2 shows the comparison of how each profile performed across four swing frequencies.

3.2.2 No Assistance Metric

Another metric of interest was how the profiles performed when measure against no assistance, wearing the exoskeleton but not providing assistive torque. The no assistance data was collected while the subject would swing their leg at each frequency while wearing the exoskeleton unpowered. Table 3 depicts the percent reductions using this metric.

TABLE 3. PERCENT REDUCTION OF NORMALIZED EMG COMPARED AGAINST SWINGING WITH AN UNPOWERED DEVICE

	80% NF	90% NF	110% NF	120% NF
RMS	-21.75%	2.12%	-13.78%	-19.13%
PKK	-9.28%	-32.66%	-30.27%	-10.19%
DISMM	-15.57%	-27.32%	-27.97%	-21.41%
RMS-PW	-20.09%	8.13%	-25.66%	-19.30%
PKK-PW	-12.28%	-32.95%	-24.09%	-20.50%
DISMM-PW	-15.69%	-9.27%	-30.12%	-21.66%

3.3 Discussion

3.3.1 Hardware vs Simulation

Averaging out all the profiles for each category leads us to observe that the hardware implementation can outperform the simulation. Simulation results average out at a reduction of 20.94% while the percent change between assisted swinging and free swinging average out to a decrease of 23.69%. However, not all hardware controllers produced a reduction in EMG activity. Few, all of the RMS derivation, produced an increase in activity. This is most likely due to the low parameters selected right below the natural frequency. The optimization likely recognized this as a region needed minimal assistance.

3.3.2 Higher Frequency vs Lower Frequency

Swinging at different frequencies was important to observe how well each type of profile could handle

variants of the activity. Since we walk at different velocities, it is an important aspect of what exoskeletons should be able to assist. Table 4 presents a comparison between low and high frequency swinging. It is an interesting note that simulation is able to generate a better performance with lower frequency than with higher frequency. On the other hand, high frequency is favorable for hardware to assist. This is perhaps due to the amount of energy it takes to swing a leg stationary at that frequency and having some level of assistance reflects higher than lower energy demanding frequencies. Further experimentation will focus on a more global metric to observe if the trend is true a scale beyond just two muscles.

TABLE 4. COMPARING EFFECTS OF LOW VS HIGH FREQUENCY

	Low Frequency	High Frequency
Simulation	-28.79%	-13.09%
No Device	-16.35%	-31.04%
Unpowered	-15.55%	-22.01%

3.3.3 Generic Work vs Positive Work

Exoskeleton assistance it typically associated with positive work exclusively. Negative work can impede with natural motion of an individual. However, allowing a small amount of negative work to achieve an objective seems to be favorable. The data in Table 5 reflects this. Implementation of general work controllers outperforms those with exclusive positive work. This can be an insightful observation for simulations that target motions that transition quickly such as leg swinging. Future work will further test the compatibility of negative work with walking controllers in hardware optimization efforts.

TABLE 5. COMPARING EFFECTS OF TYPE OF WORK ALLOWED BY OPTIMIZATION

	General Work	Positive Work
Simulation	-22.20%	-19.68%
No Device	-24.01%	-23.38%
Unpowered	-18.93%	-18.62%

3.3.4 Model Complexity

When comparing the effects of deriving a control strategy from a simple model (pendulum) vs purely a complex model (muscle model) it was found that complex is preferred (Table 6). This also has to do with the number of parameters that each control strategy uses. In future work it would be of interest to discover the threshold of where the complexity of the model (in terms of number of parameters) no longer has a defining effect on the amount of reduction. This can also be potentially circumvented by the use of optimization on a low parameter model, which ultimately was the objective of this study.

TABLE 6. COMPARING EFFECTS OF MODEL COMPLEXITY ON MUSCLE ENERGY

	Simple Pendulum	Muscle Model
Simulation	-20.33%	-22.16%
No Device	-22.58%	-25.92%
Unpowered	-17.61%	-21.13%

4. CONCLUSION

This work allowed for a side by side comparison of the implementation of discrete optimized torque profiles in both simulation and hardware. The comparison provided insight into what types of profiles might assist different swing frequencies better. This type of approach allows for versatile controllers that have more potential to be easily tuned in hardware optimization. In addition, it showed that general work can be beneficial for exoskeleton application. Future efforts will focus on experimenting on more subjects and optimizing the profiles in hardware to attempt to reduce muscle activity further.

ACKNOWLEDGEMENTS

We thank Dr. Pranav Bhounsule for the guidance and support on this project. We also thank Dr. Myunghee Kim and the Rehabilitation Robotics Laboratory at UIC for technical support.

REFERENCES

[1] Qiu, S., Pei, Z., Wang, C., and Tang, Z., 2023, "Systematic Review on Wearable Lower Extremity Robotic Exoskeletons for Assisted Locomotion," J. Bionic Eng., **20**(2), pp. 436–469.

[2] Shi, D., Zhang, W., Zhang, W., and Ding, X., 2019, "A Review on Lower Limb Rehabilitation Exoskeleton Robots," Chin. J. Mech. Eng., **32**(1), p. 74.

[3] Sanchez-Villamañan, M. del C., Gonzalez-Vargas, J., Torricelli, D., Moreno, J. C., and Pons, J. L., 2019, "Compliant Lower Limb Exoskeletons: A Comprehensive Review on Mechanical Design Principles," J. NeuroEngineering Rehabil., **16**(1), p. 55.

[4] Handford, M. L., and Srinivasan, M., 2016, "Robotic Lower Limb Prosthesis Design through Simultaneous Computer Optimizations of Human and Prosthesis Costs," Sci. Rep., **6**(1), p. 19983.

[5] Uchida, T. K., Seth, A., Pouya, S., Dembia, C. L., Hicks, J. L., and Delp, S. L., 2016, "Simulating Ideal Assistive Devices to Reduce the Metabolic Cost of Running," PLOS ONE, **11**(9), pp. 1–19.
[6] Aftabi, H., Nasiri, R., and Ahmadabadi, M. N., 2021, "Simulation-Based Biomechanical Assessment of Unpowered Exoskeletons for Running.," Sci. Rep., **11**(1), p. 11846.
[7] Dorn, T. W., Wang, J. M., Hicks, J. L., and Delp, S. L., 2015, "Predictive Simulation Generates Human Adaptations during Loaded and Inclined Walking," PLOS ONE, **10**(4), pp. 1–16.
[8] Ezati, M., Ghannadi, B., and McPhee, J., 2019, "A Review of Simulation Methods for Human Movement Dynamics with Emphasis on Gait," Multibody Syst. Dyn., **47**(3), pp. 265–292.
[9] Koelewijn, A. D., and Selinger, J. C., 2022, "Predictive Simulations to Replicate Human Gait Adaptations and Energetics With Exoskeletons," IEEE Trans. Neural Syst. Rehabil. Eng., **30**, pp. 1931–1940.
[10] Zhang, J., Fiers, P., Witte, K. A., Jackson, R. W., Poggensee, K. L., Atkeson, C. G., and Collins, S. H., 2017, "Human-in-the-Loop Optimization of Exoskeleton Assistance during Walking," Science, **356**(6344), pp. 1280–1284.
[11] Franks, P. W., Bianco, N. A., Bryan, G. M., Hicks, J. L., Delp, S. L., and Collins, S. H., 2020, "Testing Simulated Assistance Strategies on a Hip-Knee-Ankle Exoskeleton: A Case Study," *2020 8th IEEE RAS/EMBS International Conference for Biomedical Robotics and Biomechatronics (BioRob)*, pp. 700–707.
[12] Ijspeert, A. J., 2014, "Biorobotics: Using Robots to Emulate and Investigate Agile Locomotion," Science, **346**(6206), pp. 196–203.
[13] Alexander, R. M., 1989, "Optimization and Gaits in the Locomotion of Vertebrates.," Physiol. Rev., **69**(4), pp. 1199–1227.
[14] Rose, L., Bazzocchi, M. C. F., de Souza, C., Vaughan-Graham, J., Patterson, K., and Nejat, G., 2020, *A Framework for Mapping and Controlling Exoskeleton Gait Patterns in Both Simulation and Real-World*.
[15] Hess-Coelho, T. A., Cortez, M., Moura, R. T., and Forner-Cordero, A., 2022, "Progressive Improvement of the Model of an Exoskeleton for the Lower Limb by Applying the Modular Modelling Methodology," Machines, **10**(4).
[16] Aguirre-Ollinger, G., 2013, "Learning Muscle Activation Patterns via Nonlinear Oscillators: Application to Lower-Limb Assistance," *2013 IEEE/RSJ International Conference on Intelligent Robots and Systems*, pp. 1182–1189.
[17] Caillet, A. H., Phillips, A. T. M., Carty, C., Farina, D., and Modenese, L., 2022, "Hill-Type Computational Models of Muscle-Tendon Actuators: A Systematic Review," bioRxiv.
[18] Geyer, H., and Herr, H., 2010, "A Muscle-Reflex Model That Encodes Principles of Legged Mechanics Produces Human Walking Dynamics and Muscle Activities.," IEEE Trans. Neural Syst. Rehabil. Eng. Publ. IEEE Eng. Med. Biol. Soc., **18**(3), pp. 263–273.
[19] Rodrigo, S., Ambrósio, J., Silva, M., and Penisi, O., 2008, "Analysis of Human Gait Based on Multibody Formulations and Optimization Tools," Mech. Based Des. Struct. Mach., **36**, pp. 446–477.
[20] Wu, X., Xiao, L., Sun, Y., Zhang, J., Ma, T., and He, L., 2022, "A Survey of Human-in-the-Loop for Machine Learning," Future Gener. Comput. Syst., **135**, pp. 364–381.
[21] Liu, Q., Li, X., Liu, H., and Guo, Z., 2020, "Multi-Objective Metaheuristics for Discrete Optimization Problems: A Review of the State-of-the-Art," Appl. Soft Comput., **93**, p. 106382.
[22] Huang, H., Zhang, F., Hargrove, L. J., Dou, Z., Rogers, D. R., and Englehart, K. B., 2011, "Continuous Locomotion-Mode Identification for Prosthetic Legs Based on Neuromuscular-Mechanical Fusion.," IEEE Trans. Biomed. Eng., **58**(10), pp. 2867–2875.
[23] Heinemann, P., and Kasperski, M., 2017, "Damping Induced by Walking and Running," Procedia Eng., **199**, pp. 2826–2831.
[24] Plagenhoef, S., Evans, F. G., and Abdelnour, T., 1983, "Anatomical Data for Analyzing Human Motion," Res. Q. Exerc. Sport, **54**(2), pp. 169–178.